HHS Public Access

Author manuscript

Arterioscler Thromb Vasc Biol. Author manuscript; available in PMC 2019 January 01.

Published in final edited form as:

Arterioscler Thromb Vasc Biol. 2018 January ; 38(1): 83–91. doi:10.1161/ATVBAHA.117.310173.

QTL Mapping of Macrophage Cholesterol Metabolism and CRISPR/Cas9 Editing Implicate an ACAT1 Truncation as a Causal Modifier Variant

Qimin Hai[*], **Brian Ritchey**[*], **Peggy Robinet**, **Alexander M. Alzayed**, **Greg Brubaker**, **Jinying Zhang**, and **Jonathan D. Smith**

Department of Cardiology (Q.H., J.Z.), The First Affiliated Hospital of Zhengzhou University, Zhengzhou, Henan, China; Department of Cellular and Molecular Medicine (Q.H., B.R., P.R., A.M.A., G.B., J.D.S), Lerner Research Institute, Cleveland, Ohio; Department of Chemistry (B.R.), Cleveland State University, Cleveland, Ohio

Abstract

Objective—Cholesterol metabolism is a dynamic process involving intracellular trafficking, cholesterol esterification, and cholesterol ester hydrolysis. Our objective was to identify genes that regulate macrophage cholesterol metabolism.

Approaches and Results—We performed quantitative trait loci mapping of free and esterified cholesterol levels, and the ratio of esterified to free cholesterol in acetylated LDL loaded bone marrow-derived macrophages from an AKR x DBA/2 strain intercross. Ten distinct cholesterol modifier loci were identified, and bioinformatics was utilized to prioritize candidate genes. The strongest locus was located on distal chromosome 1, which we named macrophage cholesterol metabolism modifier 1 (*Mcmm1*). This locus harbors the Sterol O-acyltransferase 1 (*Soat1*) gene, encoding Acyl-Coenzyme A: cholesterol acyltransferase 1 (ACAT1), which esterifies free cholesterol. The parental AKR strain has an exon 2 deletion in *Soat1*, which leads to a 33 amino acid N-terminal truncation in ACAT1. CRISPR/Cas9 editing of DBA/2 embryonic stem cells was performed to replicate the AKR strain *Soat1* exon 2 deletion, while leaving the remainder of the genome unaltered. DBA/2 stem cells, and stem cells heterozygous and homozygous for the *Soat1* exon 2 deletion were differentiated into macrophages and loaded with acetylated LDL. DBA/2 stem cell-derived macrophages accumulated less free cholesterol and more esterified cholesterol relative to cells heterozygous and homozygous for the *Soat1* exon 2 deletion.

Conclusions—A *Soat1* deletion present in AKR mice, and resultant N-terminal ACAT1 truncation, was confirmed to be a significant modifier of macrophage cholesterol metabolism. Other *Mcmm* loci candidate genes were prioritized via bioinformatics.

Correspondence: Jonathan D. Smith, PhD, Department of Cellular and Molecular Medicine. Cleveland Clinic Lerner Research Institute, 9500 Euclid Avenue, Cleveland, Ohio. smithj4@ccf.org. Jinying Zhang, MD, PhD, Department of Cardiology. The First Affiliated Hospital of Zhengzhou University, Zhengzhou, Henan 450052, China. jyzhang@zzu.edu.cn.

[*]Authors contributed equally to this work.

Disclosures: None.

Keywords

cholesterol; cholesterol homeostasis; foam cells; macrophage; genetic association

Subject codes

Lipids and Cholesterol; Genetic; Association Studies; Functional Genomics; Information Technology; Genetics

The pathobiology of atherosclerosis is complex, but macrophage foam cells are recognized as central players.[1] Foam cells are cholesterol-laden macrophages that accumulate in the arterial intima during atherosclerosis pathology where they increase plaque burden and drive local inflammation. Foam cells store excess cholesterol as cholesterol esters (CE) in cytosolic lipid droplets, which must be hydrolyzed to unesterified, or free cholesterol (FC) in order to be effluxed from the cell.[2] In an athero-protective process known as reverse cholesterol transport, FC is effluxed to apoA1 or HDL and trafficked to the liver for processing. In the context of atherosclerosis, this process can be thought of as “macrophage reverse cholesterol transport”, as macrophages harbor the bulk of cholesterol in early lesions.[3] Foam cell CE hydrolysis is thought to be the rate-limiting step in macrophage reverse cholesterol transport.[4]

Macrophages can uptake modified forms of LDL via scavenger receptors, which are trafficked to the lysosome for degradation. After LDL degradation, FC is released from the lysosome and enters the CE cycle, with esterified cholesterol stored in LDs, which can undergo re-hydrolysis back to FC.[5] CE synthesis is catalyzed by acyl-coenzyme A:cholesterol acyltransferase (ACAT) enzymes, of which there are two isoenzymes: ACAT1 and ACAT2, encoded by the *Soat1* and *Soat2* (sterol O-acyltransferase) genes, respectively. ACAT1 is the major isoenzyme expressed in macrophages, and importantly, ACAT1 is robustly expressed in foam cells present in atherosclerotic plaque.[6] Until relatively recently, it was thought that multiple cytosolic neutral cholesterol hydrolases were responsible for CE hydrolysis, however recent studies have identified an acid hydrolase, lysosomal acid lipase, as a significant contributor to CE hydrolysis in multiple cell types including macrophages.[7] Autophagy mediates the lysosomal acid lipase-driven hydrolysis of lipid droplet CE. Work in our laboratory confirmed the role of lysosomal acid lipase and autophagy in macrophage CE hydrolysis, and further, we demonstrated that macrophage autophagic flux is impaired in athero-sensitive DBA/2 mice.[8]

Here, we employ quantitative trait locus (QTL) mapping to identify candidate genes that regulate cholesterol metabolism in bone marrow-derived macrophages (BMDMs) derived from an AKR x DBA/2 F4 strain intercross. AKR and DBA/2 mice differ substantially in their susceptibility to atherosclerosis, where DBA/2 apoE$^{-/-}$ mice develop ~ ten times larger aortic root lesions than AKR apoE$^{-/-}$ mice, and cultured BMDMs from DBA/2 vs. AKR mice accumulate much more CE after cholesterol loading with acetylated LDL (acLDL).[9] Our aim was to discover genes that play causal roles in macrophage cholesterol metabolism, which could become future targets for cardiovascular disease therapeutics. We discovered numerous macrophage cholesterol metabolism modifier (*Mcmm*) QTLs, most notably a

highly significant QTL at the distal end of chromosome 1 (*Mcmm1*) that modulates macrophage levels of FC, CE, and the CE/FC ratio after acLDL loading. *Mcmm1* harbors the *Soat1* gene. This gene has previously been shown to have a deletion in the AKR strain, leading to an N-terminal truncated ACAT1 protein, but the truncation did not alter ACAT1 activity.[10] Here we used CRISPR/Cas9 to create this *Soat1* deletion in DBA/2 embryonic stem (ES) cells. AcLDL loading studies performed on macrophages differentiated from these ES cells validated *Soat1* as the causal cholesterol metabolism modifier gene at the *Mcmm1* locus. Additionally, candidate genes at other QTLs were prioritized utilizing a combination of bioinformatics and prior BMDM cis-expression QTL (cis-eQTL) data from AKR x DBA/2 F2 crosses. Genes involved in autophagy or lysosome function were among some of the top candidates, most notably *Vps39* (vacuolar protein sorting 39), which is implicated in autophagosome-lysosome fusion.

Methods

A detailed Materials and Methods section is available in an online-only Data Supplement.

Results

A highly significant QTL for cholesterol metabolism phenotypes maps to chromosome 1

Our prior study revealed DBA/2 macrophages accumulate ~ twice as much CE as AKR cells, while AKR macrophages accumulate ~ twice as much FC after acLDL loading, amounting to an ~ 3 to 4-fold strain difference in CE/FC ratio.[8] We acLDL loaded BMDMs from 122 AKR x DBA/2 F4 mice and measured their FC and CE levels normalized to cell protein, as well as their CE/FC ratio. There was no significant effect of sex on these phenotypes, so we combined data from the male and female BMDMs. There was a broad range of FC and CE values for the F4 mice which were normally distributed (Figure 1A,B). The CE/FC ratios were not normally distributed, so a square root transformation was performed to achieve normal distribution of the data (Figure 1C). After genotyping using a high density SNP microarray (Figure I in the online-only Data Supplement), we performed QTL mapping of these BMDM cholesterol phenotypes (Figure 2).

Ten distinct macrophage cholesterol metabolism QTLs were identified, and they were named *Mcmm1–Mcmm10* (macrophage cholesterol metabolism modifier) scanning left to right across the genome in accordance with Mouse Genome Informatics nomenclature conventions (Table 1). The strongest QTL was *Mcmm1* on chromosome 1, which had the highest logarithm of the odds (LOD) scores for FC levels (LOD=10.64, peak position=155.51 Mb, mouse genome build 37), CE levels (10.76, 156.34 Mb), and CE/FC ratio (12.46, 156.35 Mb). The Bayesian credible interval (probability > 0.99 for the causal gene to reside in this interval) for CE levels at *Mcmm1* was determined to be 156.01–159.39 Mb, which was very similar to the Bayesian intervals for FC levels and CE/FC ratio. The *Mcmm1* interval replicated perfectly in an independent mapping experiment, where GC-MS was utilized to quantitate cholesterol levels, with a LOD score of 25.4 for CE/FC ratio (Figure II in the online-only Data Supplement), however it should be noted that cholesterol loading was markedly lower than usual for that experiment due to the inadvertent use of a lower concentration of acLDL. Since *Mcmm1* had the highest LOD scores for the measured

BMDM cholesterol phenotypes, *Mcmm2–Mcmm10* for CE levels were determined after correcting for *Mcmm1* genotype as an additive covariate (Figure 3).

There was a strong gene dosage effect of *Mcmm1* on FC, CE, and CE/FC ratio, with the DBA/2 allele at this locus associated with lower FC (Figure 4A), and higher CE and CE/FC ratio (Figure 4B,C). Linear regression R^2 values from these plots indicate that *Mcmm1* is associated with 30% of the variance in FC, 33% of the variance in CE, and 31% of the variance in CE/FC. Additional studies were performed to identify the *Mcmm1* causal gene.

N-terminal truncation of ACAT1 protein alters macrophage cholesterol metabolism and is causal for the Mcmm1 QTL

Mcmm1 harbors 34 genes (Table I in the online-only Data Supplement), most notably *Soat1*, which maps to 158.36 Mb. *Soat1* codes for the ACAT1 protein, an endoplasmic reticulum integral membrane protein that catalyzes esterification of FC to CE. AKR mice are known to harbor a 33 amino acid N-terminal truncation in ACAT1.[10] The Wellcome Trust Sanger Institute database documents a 6818 bp deletion (chr1:158394619–158401436) in the *Soat1* gene that extends from a site in the first intron to a site in the second intron, leading to the deletion of exon 2, which is responsible for a 118 bp mRNA deletion (Figure 5A, Figure III in the online-only Data Supplement).[11] Our prior AKR x DBA/2 strain intercross demonstrated that *Soat1* has a strong BMDM expression QTL controlled in cis (cis-eQTL) with a LOD score of 23.2, with the DBA/2 strain expressing more *Soat1* mRNA than the AKR strain.[12] We performed follow up studies on *Soat1,* the strongest *Mcmm1* candidate gene.

We first confirmed the 118 bp deletion in AKR *Soat1* mRNA. cDNA was prepared from AKR and DBA/2 BMDMs, and 3 overlapping PCR fragments were sequenced spanning the complete coding region of the C57BL/6 consensus *Soat1* mRNA sequence. The 118 bp deletion in the AKR *Soat1* cDNA was confirmed, which corresponds to exon 2 (chr1:158396812–158396929) and there were no other sequence changes in the coding region. Since exon 2 contains the translation initiation codon, the AKR ACAT1 protein translation starts at exon 3, yielding an N-terminal truncated protein missing the first 33 amino acid residues (Figure 5A).

To determine if the *Soat1* deletion is responsible for the *Mcmm1* QTL for macrophage FC, CE, and CE/FC ratio, we utilized CRISPR/Cas9 in the DBA/2 ES cell line AC173 to generate a gene deletion almost identical to the AKR *Soat1* genomic deletion. Cas9 expressing stably transfected AC173 cells were generated (Figure IV in the online-only Data Supplement) and co-transfected with two guide RNAs to generate double strand DNA breaks flanking the deletion endpoints (Figure 5B). We screened 48 clonally derived cell lines using a PCR primer set specific for the deleted allele, and a primer set specific for the DBA/2 allele. After guide RNA transfection, a pooled culture detected both the DBA/2 and deleted alleles (Figure 5C). 33 clonal lines were homozygous for the DBA/2 allele (DBA/DBA), 14 clonal cell lines were heterozygous for the DBA/2 and deleted alleles (DBA/Δ), and 1 clonal line was homozygous for the deleted allele (Δ/Δ) (Figure 5C). We sequenced a genomic PCR product from the Δ/Δ cell line that demonstrated both alleles contained the

same 6619 bp deletion spanning chr1:158394732- chr1:158401350 (Figure V in the online-only Data Supplement).

We differentiated the DBA/DBA, DBA/Δ, and Δ/Δ ES cell lines into macrophages, and ES derived macrophage (ESDM) differentiation was confirmed by uptake of DiI labeled-acLDL (Figure VI in the online-only Data Supplement). ESDMs became fully differentiated at about 13 days (Table II in the online-only Data Supplement). *Soat1* cDNA-PCR analysis demonstrated the expected 432 bp DBA allele and 314 bp Δ allele bands in DBA/DBA, DBA/Δ, and Δ/Δ ESDM cells, confirming exon 2 deletion in the edited cell lines (Figure 6A). We determined that the levels of *Soat1* mRNA were similar in the DBA/DBA and D/D ESDMs by qPCR (Figure VII in the online-only Data Supplement). We tested five commercially available ACAT1 antibodies on western blots of lysates from BMDM and ESDM, but none was specific enough to observe ACAT1 bands and show the protein truncation.

DBA/DBA, DBA/Δ, and Δ/Δ ESDMs were loaded with 50 μg/mL acLDL. Three independent cholesterol mass assay experiments revealed that the engineered 6.6 kb *Soat1* deletion significantly altered FC, CE, and CE/FC ratio. Highly significant differences were seen for FC and CE levels, where DBA/DBA ESDM accumulated significantly less FC and significantly more CE than Δ/Δ ESDM (Figure 6B,C). The DBA/DBA ESDMs had a CE/FC ratio of >2, while Δ/Δ ESDMs had a CE/FC ratio of ~ 1. The DBA/Δ ESDMs had an intermediate phenotype of ~ 1.5 (Figure 6D). The CE/FC differences for DBA/DBA vs. Δ/Δ ESDMs and DBA/Δ vs. Δ/Δ were highly significant ($p < 0.001$), as was DBA/DBA vs. DBA/Δ ($p < 0.01$). Fluorescent imaging of lipid droplets (CE) provided confirmatory evidence that the ACAT 1 N-terminal truncation decreased intracellular CE (Figure 6E–G). These data confirm that the AKR *Soat1* deletion of exon 2 is causal in manifesting the strain divergent cholesterol phenotypes at the *Mcmm1* QTL.

Candidate genes for Mcmm2 – Mcmm10

In order to prioritize candidate genes for *Mcmm2–Mcmm10*, we filtered the top candidates among all genes in these intervals (Table III in the online-only Data Supplement) for the presence of a BMDM cis-eQTL in our prior AKR x DBA/2 intercross, and/or at least one non-synonymous SNP determined to be “deleterious” by PROVEAN analysis (Table IV in the online-only Data Supplement). This left us with a group of 174 candidate genes over these 9 QTLs, some of which were associated with cholesterol, autophagy, lysosome, and atherosclerosis in PubMed queries. We cross-referenced the top 174 candidate genes for *Mcmm2 – Mcmm10* plus the 34 genes in the *Mcmm1* QTL to the human genome wide association catalog for atherosclerosis relevant traits such as cholesterol, lipoproteins, and coronary artery disease. We found genome wide association study matches for the human genes CACNA1E, CST3, DSTN, LRP4, MACROD2, SNX5, MEPE, APOBEC1, STAB2, UTP20, CAMK2B, EHBP1, NPC1L1, PELI1, and DYNC2LI1 (Table V in the online-only Data Supplement).

Mcmm3 is located on chromosome 2 and has a very large Bayesian credible interval of 76.28–180.09 Mb that harbors 2,223 genes. While this locus is quite large, it is very interesting because it may harbor distinct proximal (near 120 Mb) and distal (near 158 Mb)

loci (Figure 3). It contains many plausible candidate genes, and it partially overlaps *Ath28,* an atherosclerosis modifier locus we discovered in prior AKR x DBA/2 intercrosses.[12] *Vps39* and *Mertk* are our top candidates for the proximal region. *Lbp* and *Bpi* are our top candidates for the distal region. The remaining *Mcmm* QTL candidate genes are discussed in the online-only Data Supplement.

Discussion

Ten macrophage cholesterol metabolism QTLs were discovered from our AKR x DBA/2 strain intercross. The *Mcmm1* QTL on distal chromosome 1 had the highest LOD scores for FC, CE, and CE/FC ratio and it replicated in an independent experiment. Of the 34 genes in this interval, *Soat1*, encoding ACAT1, was our top causal candidate gene, which we confirmed as the causal gene by CRISPR/Cas9 gene editing in DBA/2 ES cells. As with any QTL, this does not rule out the possibility that other genes in *Mcmm1* may also contribute to these phenotypes. ACAT1 is expressed in many tissues, including macrophages, whereas its isoenzyme, ACAT2 (coded for by the *Soat2* gene), is expressed almost exclusively in intestinal epithelial cells and hepatocytes. Our prior transcriptomic study showed high expression of *Soat1* and low expression of *Soat2* in BMDMs from these strains.[13] ACAT1 and ACAT2 share sequence homology near the C-terminus, however they differ significantly near the N-terminus in both mouse and human.[14] AKR mice are known to harbor a 33 amino acid N-terminal truncation in ACAT1 due to a 6.8kb genomic deletion in *Soat1*. The ACAT1 protein truncation in AKR mice was first discovered by Farese and colleagues, but they demonstrated that the truncated ACAT1 protein did not have diminished esterification activity.[10] Similarly, our prior study of BMDMs from AKR and DBA/2 mice did not demonstrate a difference in ACAT activity.[8] However, based on our current findings, the ACAT activity assay may not be reflective of cellular cholesterol esterification. Two in-vivo phenotypes have been ascribed to the ACAT1 truncation in AKR mice; adrenocortical lipid depletion (*ald*), and hair interior defect (*hid*). The *ald* phenotype results in a loss of cholesterol esters in the adrenal cortex of post-pubescent AKR mice, which is much more pronounced in males than females.[10] The hair interior defect results in the absence of ACAT1 expression in the premedulla, sebaceous glands, and hair interior of hair follicles.[11]

Inhibition of ACAT enzymes has long been recognized as an attractive therapeutic target for cardiovascular disease, and ACAT inhibitors have shown efficacy in reducing atherosclerosis in mouse models.[15, 16] However, *Soat1*$^{-/-}$ mice did not show a reduction in atherosclerosis on either *apoE*$^{-/-}$ or *Ldlr*$^{-/-}$ backgrounds, and these mice had massive xanthomatosis.[17] Furthermore, *Ldlr*$^{-/-}$ mice with macrophage specific deletion of *Soat1* had an unanticipated increase in atherosclerosis.[18] It is worth noting that AKR mice on the *apoE*$^{-/-}$ background do not have xanthomas, and thus the AKR *Soat1* allele with its N-terminal ACAT1 protein truncation is not a phenocopy of the knockout allele. Theoretically, non-specific ACAT inhibitors could have dual athero-protective effects, where inhibition of ACAT1 would decrease foam cell formation, and inhibition of ACAT2 would decrease cholesterol uptake and LDL production. Unfortunately, ACAT inhibitor trials in humans have not shown efficacy in reducing plaque burden or attenuating adverse cardiac events in three independent phase 3 clinical trials, with macrophage FC toxicity posited as a primary reason for the disappointing results.[19–21] In these trials the ACAT inhibitors acted on both ACAT1

and ACAT2. Additionally, in all three studies there was an unanticipated rise in LDL-C in treatment groups, and a positive correlation between LDL-C levels and treatment dosage. Therefore, potential anti-atherogenic effects of ACAT inhibitors may be partly offset by the rise in LDL-C levels. Still, these trials cast significant doubt on the prospects of targeting ACAT enzymes as a cardiovascular disease therapeutic.

In 2007, the first selective ACAT1 inhibitor (K-604) was developed, which showed over 200-fold affinity for ACAT1 vs. ACAT2, and decreased atherosclerosis in hamster models.[22] K-604 was also shown to favorably alter atherosclerotic plaque phenotypes in apoE$^{-/-}$ mice.[23] Additionally, this compound was shown to be effective in ameliorating symptoms of Alzheimer's disease in mouse models, where K-604 treatment was shown to increase autophagic flux and transcription factor EB -mediated lysosome biogenesis in cultured microglia cells.[24] This raises the interesting prospect that the rise in intracellular FC caused by the ACAT1 truncation in AKR macrophages may also result in the induction of autophagy and/or autophagosome-lysosome fusion, as cholesterol-enriched autophagosomes may have enhanced ability to fuse with lysosomes.[25] Our results suggest that small molecules that interact with the N-terminus of ACAT1 may decrease CE accumulation and might be worth pursuing as a cardiovascular disease therapeutic.

Our lab has previously demonstrated that DBA/2 BMDM foam cells have diminished autophagic flux vs. AKR BMDM foam cells, which may contribute to the decreased CE turnover and increased CE storage in the DBA/2 strain.[8] We specifically observed decreased autophagosome fusion with lysosomes in the DBA/2 cells.[8] Based on these data, genes involved in autophagy and lysosome function were expected to appear in our QTL intervals. *Vps39* (vacuolar protein sorting 39) maps very close to the *Mcmm3* peak LOD marker on chromosome 2 and is one of our top candidate genes at this locus (Supplemental Table III in the online-only Data Supplement). *Vps39* has a strong BMDM cis-eQTL with a LOD score of 12.9, and its expression is higher in AKR BMDMs than DBA/2. This protein is part of the homotypic fusion and protein-sorting complex that has been shown to mediate autophagosome-lysosome fusion in cultured cells, and siRNA knockdown of *Vps39* blocked autophagic flux.[26] Thus, its lower expression in DBA/2 BMDM coincides with decreased autophagic flux.

Prior studies in our laboratory revealed atherosclerosis modifier loci on chromosomes 2 (*Ath28*), 15 (*Ath22*), and 17 (*Ath26*) for an AKR x DBA/2 strain intercross.[12] Given the centrality of foam cells to atherosclerosis pathology, we anticipated that the *Mcmm* QTLs might overlap our Ath QTLs and aid in prioritizing *Ath* candidate genes. *Mcmm3* on chromosome 2 (76.28–180.09 Mb) partially overlaps *Ath28* (165.1–179.3 Mb), and thus determination of the causal gene for *Mcmm3* could suggest the causal gene for *Ath28*. A recent study identified a chromosome 2 atherosclerosis QTL (*Aath4,* 123–148 Mb) in a 129S6 x DBA/2 backcross that contains the *Mertk* gene, which is another of our top candidates for the *Mcmm3* QTL (Supplemental Table III in the online-only Data Supplement). The study demonstrated that reduced *Mertk* expression in DBA/2 macrophages led to decreased efferocytosis, which is a plausible mechanism that could contribute to increased atherosclerosis in DBA/2 mice.[27] Prior studies in *apoE*$^{-/-}$ and *Ldlr*$^{-/-}$ mice have demonstrated that *Mertk* loss of function mutations increased lesion necrotic core

area with increased apoptotic cells, and led to larger lesions in the *Ldlr*$^{-/-}$ background.[28] *Mertk* had a strong BMDM cis-eQTL in our AKR x DBA/2 intercross.[12] However, the *Ath28* QTL does not contain the *Mertk* gene, so if this proves to be a causal modifier gene for *Mcmm3*, it would not explain the *Ath28* QTL. Two *Mcmm3* top candidates genes are found within the *Ath28* interval, *Zfp663* and *Cstf1* (Supplemental Table III in the online-only Data Supplement).

At the more distal end of chromosome 2, *Lbp* (lipopolysaccharide binding protein) is an interesting *Mcmm3* candidate. *Lbp* had a BMDM cis-eQTL in our prior study, with higher expression in DBA/2 vs. AKR BMDMs. Additionally, *Lbp* harbors 3 non-synonymous SNPs between the strains, one of which (Y284H) is predicted to be deleterious by PROVEAN software. Distal chromosome 2 displayed a robust QTL (*Ath45*, 157–165 Mb) for aortic root lesion size in an F2 cross of DBA/2 x 129S6 apoE$^{-/-}$ mice[29], partially overlapping the *Ath28* QTL. The investigators cite *Lbp* as a top candidate for *Ath45*, noting that the Y285H SNP (which occurs in the 129S6 strain) is located in a conserved lipid binding site, whose alteration may affect protein function. *Lbp* was recently shown to increase macrophage LXR activity and promote macrophage survival and atherosclerosis in *Ldlr*$^{-/-}$ mice[30] Another interesting aspect of the LBP protein is that is shares structural similarity to cholesterol ester transfer protein (CETP) and phospholipid transfer protein (PLTP), raising the distinct possibility that LBP may bind more lipid species than just LPS, e.g. phospholipids.[31] Additionally, LBP was recently identified as a novel, plaque derived biomarker of atheroma released rapidly after plaque disruption.[32] The gene encoding bactericidal permeability increasing protein (*Bpi*) maps just distal to *Lbp*, and also shares structural similarity with CETP, PLTP, and LBP. *Bpi* has 4 non-synonymous SNPs between AKR and DBA/2, one of which was predicted to be deleterious by PROVEAN. It is of interest that a top candidate for *Mcmm2* QTL is the *Tlr5* gene, which along with *Lpb* and *Bpi* is another gene related to pathogen-associated molecular pattern (PAMP) function, suggesting that there may be an interaction between PAMP signaling and cholesterol metabolism that remains to be elucidated.

Our study demonstrated that the 33 amino acid N-terminal ACAT1 truncation in AKR mice plays a significant causal role in macrophage cholesterol metabolism. How this truncation affects cholesterol metabolism remains unknown, but altered protein-protein and/or protein-lipid interactions is a plausible mechanism. Since we did not detect an effect of the ACAT1 truncation on *Soat1* mRNA levels in our engineered ESDMs, additional genetic differences between the AKR and DBA/2 *Soat1* locus must be responsible for the *Soat1* eQTL that we previously reported.[13] Bioinformatic analysis of other *Mcmm* loci suggest that *Vps39*, *Lbp*, and other candidate genes are worthy of follow up study to interrogate their potential role in macrophage cholesterol metabolism.

Supplementary Material

Refer to Web version on PubMed Central for supplementary material.

Acknowledgments

We thank Joshua N. Phelps for technical assistance with the embryonic stem cell-derived macrophages.

Sources of Funding: This study was supported by NIH grant P01HL029582. Q.H. was supported by the China Scholarship Council.

Nonstandard Abbreviations

ACAT	acyl-coenzyme A:cholesterol acyltransferase
AcLDL	acetylated low density lipoprotein
BMDM	bone marrow-derived macrophage
CE	cholesterol ester
eQTL	expression quantitative trait locus
ES	embryonic stem
ESDM	embryonic stem cell-derived macrophage
FC	free cholesterol
LOD	logarithm of the odds
MCMM	macrophage cholesterol metabolism modifier
QTL	quantitative trait locus
SOAT	sterol O-acyltransferase

Reference List

1. Moore KJ, Tabas I. Macrophages in the pathogenesis of atherosclerosis. Cell. 2011; 145:341–55. [PubMed: 21529710]
2. Libby P, Ridker PM, Hansson GK. Progress and challenges in translating the biology of atherosclerosis. Nature. 2011; 473:317–25. [PubMed: 21593864]
3. Cuchel M, Rader DJ. Macrophage reverse cholesterol transport: key to the regression of atherosclerosis? Circulation. 2006; 113:2548–55. [PubMed: 16735689]
4. Sakai K, Igarashi M, Yamamuro D, Ohshiro T, Nagashima S, Takahashi M, Enkhtuvshin B, Sekiya M, Okazaki H, Osuga J, Ishibashi S. Critical role of neutral cholesteryl ester hydrolase 1 in cholesteryl ester hydrolysis in murine macrophages. J Lipid Res. 2014; 55:2033–40. [PubMed: 24868095]
5. Brown MS, Ho YK, Goldstein JL. The cholesteryl ester cycle in macrophage foam cells. Continual hydrolysis and re-esterification of cytoplasmic cholesteryl esters. J Biol Chem. 1980; 255:9344–52. [PubMed: 7410428]
6. Miyazaki A, Sakashita N, Lee O, Takahashi K, Horiuchi S, Hakamata H, Morganelli PM, Chang CC, Chang TY. Expression of ACAT-1 protein in human atherosclerotic lesions and cultured human monocytes-macrophages. Arterioscler Thromb Vasc Biol. 1998; 18:1568–74. [PubMed: 9763528]
7. Ouimet M, Franklin V, Mak E, Liao X, Tabas I, Marcel YL. Autophagy regulates cholesterol efflux from macrophage foam cells via lysosomal acid lipase. Cell Metab. 2011; 13:655–67. [PubMed: 21641547]
8. Robinet P, Ritchey B, Smith JD. Physiological difference in autophagic flux in macrophages from 2 mouse strains regulates cholesterol ester metabolism. Arterioscler Thromb Vasc Biol. 2013; 33:903–10. [PubMed: 23493286]

9. Smith JD, Bhasin JM, Baglione J, Settle M, Xu Y, Barnard J. Atherosclerosis susceptibility loci identified from a strain intercross of apolipoprotein E-deficient mice via a high-density genome scan. Arterioscler Thromb Vasc Biol. 2006; 26:597–603. [PubMed: 16373612]
10. Meiner VL, Welch CL, Cases S, Myers HM, Sande E, Lusis AJ, Farese RV Jr. Adrenocortical lipid depletion gene (ald) in AKR mice is associated with an acyl-CoA:cholesterol acyltransferase (ACAT) mutation. J Biol Chem. 1998; 273:1064–9. [PubMed: 9422770]
11. Wu B, Potter CS, Silva KA, Liang Y, Reinholdt LG, Alley LM, Rowe LB, Roopenian DC, Awgulewitsch A, Sundberg JP. Mutations in sterol O-acyltransferase 1 (Soat1) result in hair interior defects in AKR/J mice. J Invest Dermatol. 2010; 130:2666–8. [PubMed: 20574437]
12. Hsu J, Smith JD. Genetic-genomic replication to identify candidate mouse atherosclerosis modifier genes. J Am Heart Assoc. 2013; 2:e005421. [PubMed: 23525445]
13. Berisha SZ, Hsu J, Robinet P, Smith JD. Transcriptome analysis of genes regulated by cholesterol loading in two strains of mouse macrophages associates lysosome pathway and ER stress response with atherosclerosis susceptibility. PLoS One. 2013; 8:e65003. [PubMed: 23705026]
14. Chang TY, Li BL, Chang CC, Urano Y. Acyl-coenzyme A:cholesterol acyltransferases. Am J Physiol Endocrinol Metab. 2009; 297:E1–E9. [PubMed: 19141679]
15. Kusunoki J, Hansoty DK, Aragane K, Fallon JT, Badimon JJ, Fisher EA. Acyl-CoA:cholesterol acyltransferase inhibition reduces atherosclerosis in apolipoprotein E-deficient mice. Circulation. 2001; 103:2604–9. [PubMed: 11382731]
16. Rong JX, Blachford C, Feig JE, et al. ACAT inhibition reduces the progression of preexisting, advanced atherosclerotic mouse lesions without plaque or systemic toxicity. Arterioscler Thromb Vasc Biol. 2013; 33:4–12. [PubMed: 23139293]
17. Accad M, Smith SJ, Newland DL, Sanan DA, King LE Jr, Linton MF, Fazio S, Farese RV Jr. Massive xanthomatosis and altered composition of atherosclerotic lesions in hyperlipidemic mice lacking acyl CoA:cholesterol acyltransferase 1. J Clin Invest. 2000; 105:711–9. [PubMed: 10727439]
18. Fazio S, Major AS, Swift LL, Gleaves LA, Accad M, Linton MF, Farese RV Jr. Increased atherosclerosis in LDL receptor-null mice lacking ACAT1 in macrophages. J Clin Invest. 2001; 107:163–71. [PubMed: 11160132]
19. Tardif JC, Gregoire J, L'Allier PL, et al. Effects of the acyl coenzyme A:cholesterol acyltransferase inhibitor avasimibe on human atherosclerotic lesions. Circulation. 2004; 110:3372–7. [PubMed: 15533865]
20. Nissen SE, Tuzcu EM, Brewer HB, Sipahi I, Nicholls SJ, Ganz P, Schoenhagen P, Waters DD, Pepine CJ, Crowe TD, Davidson MH, Deanfield JE, Wisniewski LM, Hanyok JJ, Kassalow LM. Effect of ACAT inhibition on the progression of coronary atherosclerosis. N Engl J Med. 2006; 354:1253–63. [PubMed: 16554527]
21. Meuwese MC, de GE, Duivenvoorden R, Trip MD, Ose L, Maritz FJ, Basart DC, Kastelein JJ, Habib R, Davidson MH, Zwinderman AH, Schwocho LR, Stein EA. ACAT inhibition and progression of carotid atherosclerosis in patients with familial hypercholesterolemia: the CAPTIVATE randomized trial. JAMA. 2009; 301:1131–9. [PubMed: 19293413]
22. Ikenoya M, Yoshinaka Y, Kobayashi H, Kawamine K, Shibuya K, Sato F, Sawanobori K, Watanabe T, Miyazaki A. A selective ACAT-1 inhibitor, K-604, suppresses fatty streak lesions in fat-fed hamsters without affecting plasma cholesterol levels. Atherosclerosis. 2007; 191:290–7. [PubMed: 16820149]
23. Yoshinaka Y, Shibata H, Kobayashi H, Kuriyama H, Shibuya K, Tanabe S, Watanabe T, Miyazaki A. A selective ACAT-1 inhibitor, K-604, stimulates collagen production in cultured smooth muscle cells and alters plaque phenotype in apolipoprotein E-knockout mice. Atherosclerosis. 2010; 213:85–91. [PubMed: 20843517]
24. Shibuya Y, Niu Z, Bryleva EY, Harris BT, Murphy SR, Kheirollah A, Bowen ZD, Chang CC, Chang TY. Acyl-coenzyme A:cholesterol acyltransferase 1 blockage enhances autophagy in the neurons of triple transgenic Alzheimer's disease mouse and reduces human P301L-tau content at the presymptomatic stage. Neurobiol Aging. 2015; 36:2248–59. [PubMed: 25930235]
25. Shibuya Y, Chang CC, Chang TY. ACAT1/SOAT1 as a therapeutic target for Alzheimer's disease. Future Med Chem. 2015; 7:2451–67. [PubMed: 26669800]

26. Jiang P, Nishimura T, Sakamaki Y, Itakura E, Hatta T, Natsume T, Mizushima N. The HOPS complex mediates autophagosome-lysosome fusion through interaction with syntaxin 17. Mol Biol Cell. 2014; 25:1327–37. [PubMed: 24554770]

27. Kayashima Y, Makhanova N, Maeda N. DBA/2J Haplotype on Distal Chromosome 2 Reduces Mertk Expression, Restricts Efferocytosis, and Increases Susceptibility to Atherosclerosis. Arterioscler Thromb Vasc Biol. 2017; 37:e82–e91. [PubMed: 28473436]

28. Kayashima Y, Makhanova NA, Matsuki K, Tomita H, Bennett BJ, Maeda N. Identification of aortic arch-specific quantitative trait loci for atherosclerosis by an intercross of DBA/2J and 129S6 apolipoprotein E-deficient mice. PLoS One. 2015; 10:e0117478. [PubMed: 25689165]

29. Kayashima Y, Tomita H, Zhilicheva S, Kim S, Kim HS, Bennett BJ, Maeda N. Quantitative trait loci affecting atherosclerosis at the aortic root identified in an intercross between DBA2J and 129S6 apolipoprotein E-null mice. PLoS One. 2014; 9:e88274. [PubMed: 24586312]

30. Sallam T, Ito A, Rong X, Kim J, van SC, Chamberlain BT, Jung ME, Chao LC, Jones M, Gilliland T, Wu X, Su GL, Tangirala RK, Tontonoz P, Hong C. The macrophage LBP gene is an LXR target that promotes macrophage survival and atherosclerosis. J Lipid Res. 2014; 55:1120–30. [PubMed: 24671012]

31. Alva V, Lupas AN. The TULIP superfamily of eukaryotic lipid-binding proteins as a mediator of lipid sensing and transport. Biochim Biophys Acta. 2016; 1861:913–23. [PubMed: 26825693]

32. Lee R, Fischer R, Charles PD, Adlam D, Valli A, Di GK, Kharbanda RK, Choudhury RP, Antoniades C, Kessler BM, Channon KM. A novel workflow combining plaque imaging, plaque and plasma proteomics identifies biomarkers of human coronary atherosclerotic plaque disruption. Clin Proteomics. 2017; 14:22. [PubMed: 28642677]

Highlights

- Ten distinct macrophage cholesterol metabolism modifier (*Mcmm*) loci were identified in our AKR x DBA/2 F4 intercross association mapping study.
- A *Soat1* exon 2 deletion, and the resultant ACAT1 N-terminal truncation, was unequivocally verified as a significant modulator of macrophage cholesterol metabolism via QTL mapping and CRISPR/Cas9 gene editing.
- Bioinformatic analyses of the *Mcmm* loci prioritized candidate genes and highlighted several genes worthy of follow up study such as *Vps39* and *Lbp*.

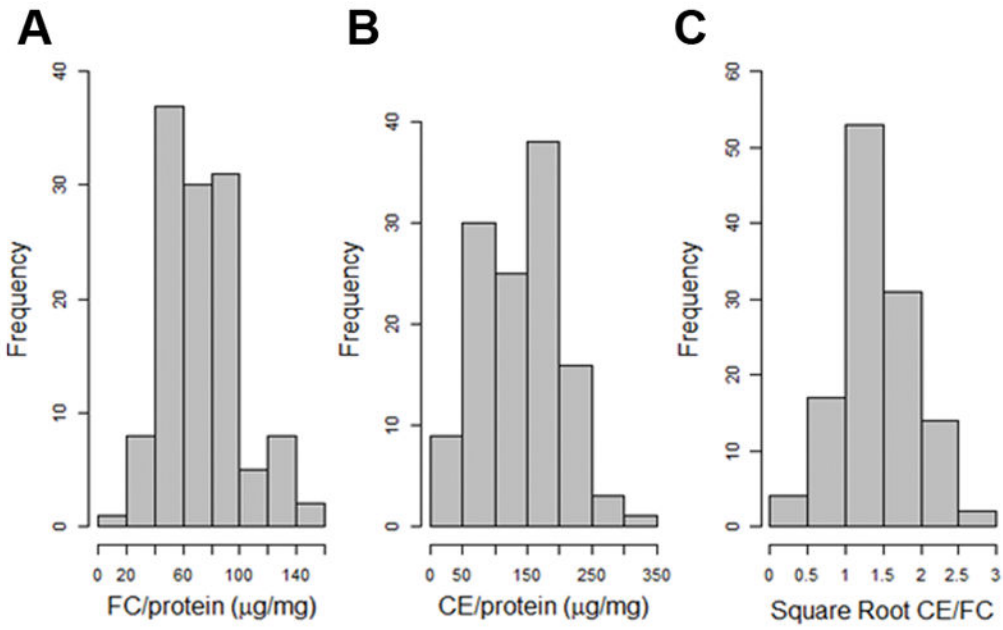

Figure 1.

Frequency histograms of cholesterol phenotypes for BMDMs derived from 122 F4 mice after loading with 50µg/mL acLDL. **A,** FC normalized to cellular protein. **B,** CE normalized to cellular protein. **C,** CE/FC data was not normally distributed, so a square root transformation was performed to achieve a normal distribution.

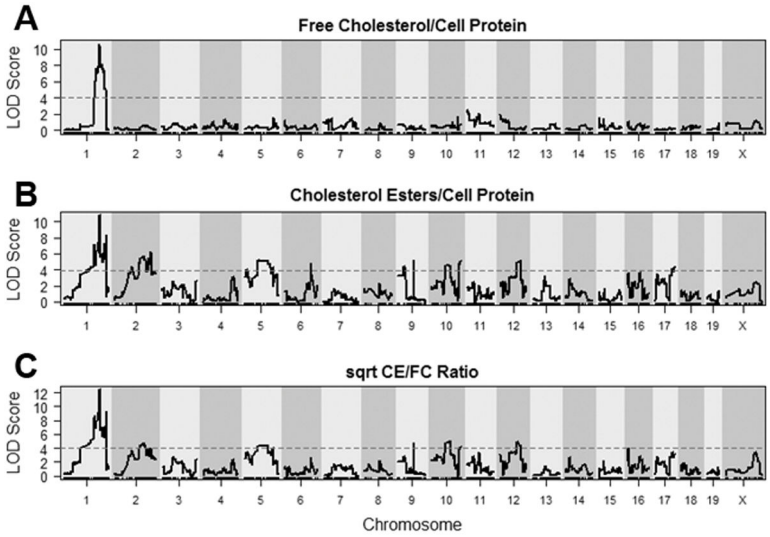

Figure 2.

LOD plots for cholesterol phenotypes. **A**, FC; **B**, CE; and **C**, Square root transformed CE/FC. Dashed lines represent genome-wide significance thresholds ($\alpha = 0.05$) determined by permutation analysis.

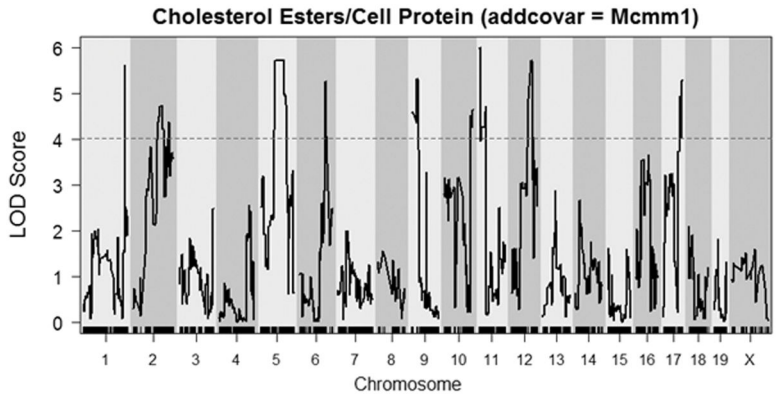

Figure 3.

LOD plot for CE after correcting for the *Mcmm1* peak marker as an additive covariate. The dashed line represents the genome-wide significance threshold ($\alpha = 0.05$) determined by permutation analysis.

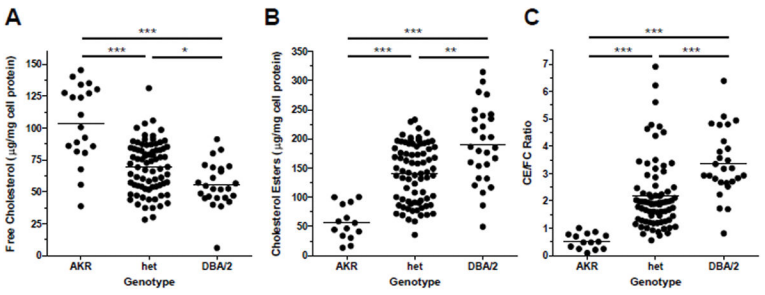

Figure 4.

Gene dose response plots for *Mcmm1* cholesterol phenotypes. **A,** FC for three groups separated by genotype at *Mcmm1* (R^2 = 0.30, β = −23.4 μg FC/mg cellular protein). **B,** CE (R^2 = 0.33, β = 62.9 μg CE/mg cellular protein). **C,** CE/FC (R^2 = 0.31, β = 1.37). *, p<0.05; **, p<0.01; ***, p<0.001 by non-parametric Kruskal-Wallis ANOVA posttest. Circles represent individual F4 mice, lines represent the mean phenotype value for the specified genotype.

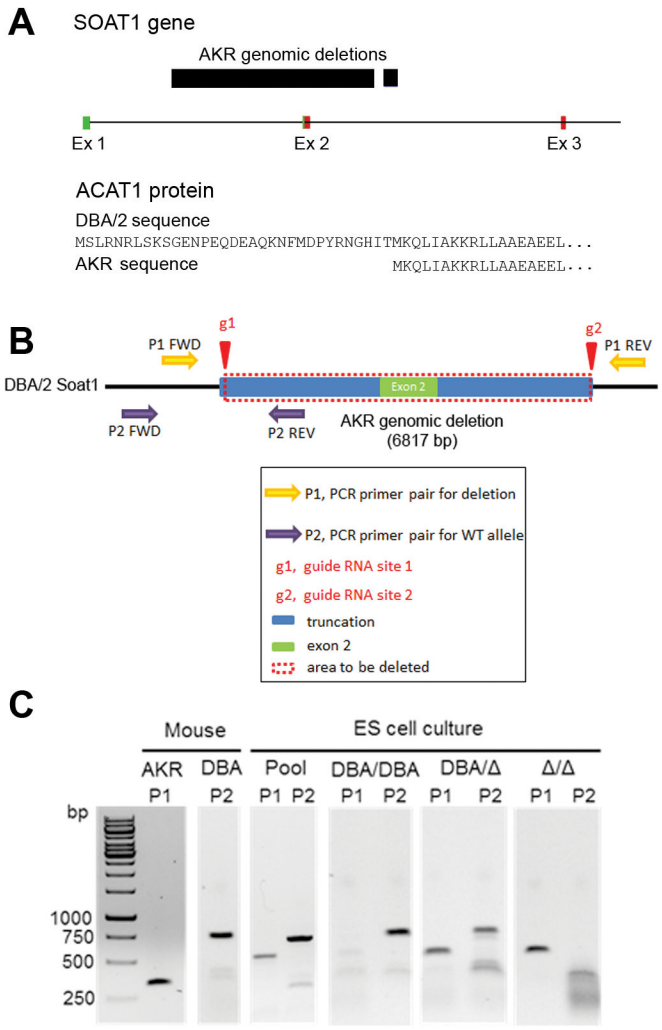

Figure 5.

A, AKR *Soat1* genomic deletion and ACAT1 N-terminal truncation. AKR mice have a 6.8kb genomic deletion that spans exon 2, leading to a 33 amino acid ACAT1 N-terminal truncation. Green boxes, exonic 5′-UTR; red boxes, exonic coding sequence. **B,** Pictorial representation of *Soat1* CRISPR/Cas9 deletion strategy for DBA/2 ES cells. **C,** Genomic DNA PCR confirming the *Soat1* deletion in AKR BMDMs, and showing the expected bands for DBA/DBA, DBA/Δ, and Δ/Δ ES cells.

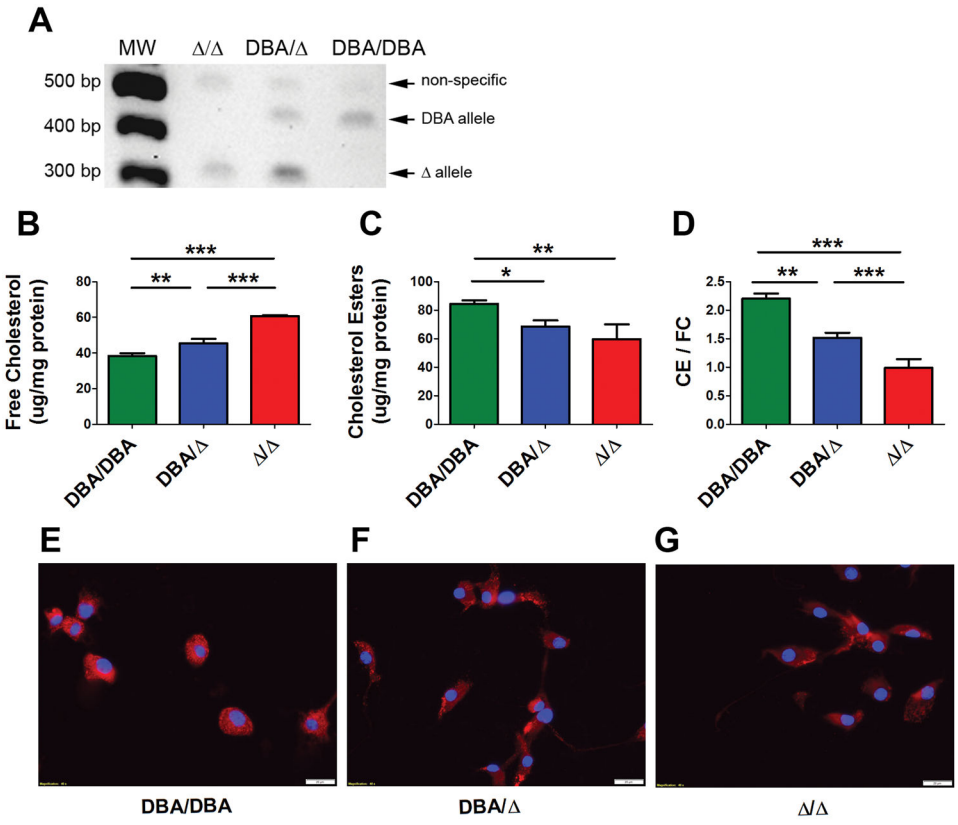

Figure 6.

A, cDNA-PCR from DBA/DBA, DBA/Δ, and Δ/Δ ESDMs using primers in exons 1 and 4 showing expected *Soat1* mRNA bands. **B–D,** Comparison of cholesterol phenotypes between the three ESDM genotypes after loading with 50μg/mL acLDL. *, $p<0.05$; **, $p<0.01$; ***, $p<0.001$ by Newman-Keuls Multiple Comparison Test; n=3 ± S.D. Figure is representative of 3 independent experiments. **E–G,** ESDMs were loaded with 50μg/mL acLDL. More CE accumulation was observed per DBA/2 allele. Blue, DAPI-stained nuclei, red, Nile Red-stained neutral lipids, 40× magnification (white bar = 20μm).

Table 1

Macrophage cholesterol metabolism modifier QTLs

QTL name	Trait	Chromosome	Interval in Mb (peak)	Max LOD score	p-value
Mcmm1	FC	1	155.35–159.40 (155.51)	10.6	< **0.0001**
Mcmm1	CE	1	156.01–159.39 (156.34)	10.8	< **0.0001**
Mcmm1	CE/FC	1	155.99–159.34 (156.35)	12.5	< **0.0001**
Mcmm2*	CE	1	184.65–184.89 (184.65)	5.6	< **0.01**
Mcmm2*	CE/FC	1	184.65–184.89 (184.65)	6.1	< **0.01**
Mcmm3*	CE	2	76.28–180.10 (118.97)	4.7	< **0.05**
Mcmm3*	CE/FC	2	74.98–180.10 (126.97)	3.5	< 0.20
Mcmm4*	CE	5	68.02–107.43 (105.44)	5.7	< **0.01**
Mcmm4*	CE/FC	5	68.02–107.39 (105.44)	4.6	< **0.05**
Mcmm5*	CE	6	118.95–122.59 (120.13)	5.3	< **0.01**
Mcmm5*	CE/FC	6	5.50–149.04 (120.13)	2.4	> 0.63
Mcmm6*	CE	9	3.58–34.82 (31.70)	5.3	< **0.01**
Mcmm6*	CE/FC	9	3.58–34.82 (31.19)	3.6	= 0.15
Mcmm7*	CE	10	6.41–129.61 (127.52)	4.6	< **0.05**
Mcmm7*	CE/FC	10	3.21–129.61 (17.54)	3.9	< 0.10
Mcmm8*	CE	11	4.03–36.44 (7.27)	6.0	< **0.01**
Mcmm8*	CE/FC	11	4.03–58.93 (4.03)	3.8	< 0.10
Mcmm9*	CE	12	79.09–95.60 (95.60)	5.7	< **0.01**
Mcmm9*	CE/FC	12	45.53–103.96 (80.45)	4.8	< **0.05**
Mcmm10*	CE	17	68.68–89.29 (88.56)	5.3	< **0.01**
Mcmm10*	CE/FC	17	13.63–89.29 (77.30)	3.8	< 0.15

*, Values determined after correcting for *Mcmm1* as an additive covariate